# Do Probe Molecules Influence Water in Confinement?

**Bharat Baruah, Laura A. Swafford, Debbie C. Crans,* and Nancy E. Levinger***

*Department of Chemistry, Colorado State University, Colorado 80523-1872*

*Received: January 15, 2008; Revised Manuscript Received: April 30, 2008*

The water inside reverse micelles can differ dramatically from bulk water. Some changes in properties can be attributed to the interaction of water molecules with the micellar interface, forming a layer of shell water inside the reverse micelle. The work reported here monitors changes in intramicellar water through chemical shifts and signal line widths in $^{51}$V NMR spectra of a large polyoxometalate probe, decavanadate, and from infrared spectroscopy of isotopically labeled water, to obtain information on the water in the water pool in AOT reverse micelles formed in isooctane. The studies reveal several things about the reverse micellar water pool. First, in agreement with our previous measurements, the proton equilibrium of the decavanadate solubilized within the reverse micelles differs from that in bulk aqueous solution, indicating a more basic environment compared to the starting stock solutions from which the reverse micelles were formed. Below a certain size, reverse micelles do not form when the polyoxometalate is present; this indicates that the polyanionic probe requires a layer of water to solvate it in addition to the water that solvates the surfactant headgroups. Finally, the polyoxometalate probe appears to perturb the water hydrogen-bonding network in a fashion similar to that in the interior surface of the reverse micelles. These measurements demonstrate the dramatic differences possible for water environments in confined spaces.

## I. Introduction

Self-assembled molecular structures such as reverse micelles (RMs) are convenient and tunable nanoscale structures that offer researchers new and different environments for chemistry, biology, and beyond. These nanoscale droplets of water form when a surfactant layer sequesters the aqueous phase from a bulk nonpolar liquid phase. These minuscule pockets of water have been used to study enzymatic reactions,[1–5] catalytic reactions,[6–11] and interface activity[12–14] in a confined environment. Motion of molecules in confined environments affects the properties of molecules and thereby can impact reactions. Thus, fundamental information on how confinement impacts molecular properties is important in a wide range of fields across a broad range of science disciplines.

Researchers continue to explore the properties of the water in the interior of RMs, often employing probe molecules to report on RM properties. Through a wide range of experiments and simulations, we know that water molecules inside the RM behave differently than they do in bulk solution.[15–24] The distinction of the two types of water most likely reflects the various interactions of water with the surfactant head groups and the counter cations.[25] Reporter probe molecules have also been enlisted to investigate the properties of water inside the RMs. By using fluorescent probes, we[18,26] and others[27] have found that the RM interior slows solvation dynamics. Heitz and Bright found increased microviscosity inside RMs.[28] In contrast, by using time-resolved IR studies, Sando et al. found relatively small, if any, differences for vibrational energy relaxation for azide in RMs.[29] Direct probes of intramicellar water, by using steady-state and time-resolved IR spectroscopy, have determined that hydrogen bonding of the water molecules near the surfactant interface differs from that of water in the micellar core.[24,30]

* Corresponding authors. E-mail: Debbie.Crans@ColoState.edu and Nancy.Levinger@ColoState.edu.

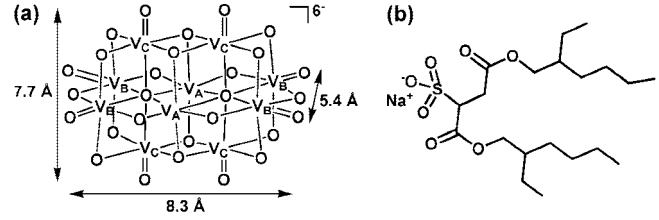


**Figure 1.** Structures of (a) $[V_{10}O_{28}]^{6-}$ ($V_{10}$) and (b) AOT.

Recently, we have demonstrated the efficacy of vanadium oxometalates as probes of the RM interior.[31–33] The highly charged inorganic molecule, decavanadate, $V_{10}$ ($[V_{10}O_{28}]^{6-}$), is highly water soluble (Figure 1). $V_{10}$ is thermodynamically stable in aqueous solution with pH from 3 to 6.[34,35] Although not thermodynamically stable above pH 6, $V_{10}$ can persist for a few days because of its very slow hydrolysis to other vanadate oligomers. In $V_{10}$, vanadium atoms experience one of three different locations. Two atoms reside in equatorial sites, labeled $V_A$, whereas four vanadium atoms each can be found in equatorial $V_B$ and axial $V_C$ sites, as shown in Figure 1. Each vanadium atom is bound to six oxygen atoms in a slightly distorted octahedral environment. The high charge and compact form of the molecule lead it to reside comfortably in the interior water pool of most of the RMs we have explored.[31]

In the work reported here, we present results from experiments exploring the influence of decavanadate on the nature of the intramicellar aqueous pools in Aerosol OT (AOT) RMs. The AOT RMs investigated form in isooctane as the nonpolar organic solvent. We vary the size of the water pool by changing the relative amount of aqueous solution to surfactant, $w_0$ = [$H_2O$]/[surfactant]. As $w_0$ increases, the amount of water in the RM core increases, whereas the shell water layer remains nearly the same.[25] We use $^{51}$V NMR to follow chemical shifts, line broadening, and relaxation times of the $V_{10}$ in the RMs as well as steady-state IR spectroscopy of isotopically labeled water to

10.1021/jp800390t CCC: $40.75 
Published on Web 07/24/2008

measure the impact of the $V_{10}$ on the water. Line broadening in the NMR spectra indicates substantial changes in the $V_{10}$ mobility as the RM size decreases, suggesting fundamental changes in the nature of the water inside the RMs. IR spectroscopy allows us to explore the hydrogen bonding in the intramicellar water. Taken together, results indicate substantial differences for water in the RMs in the presence of the large oxometalate probe.

## II. Experimental Methods

**II.A. Materials.** Sodium metavanadate, $NaVO_3$ (99.9%) and AOT (sodium bis(2-ethylhexyl)sulfosuccinate or docusate sodium salt, 99%) were purchased from Sigma-Aldrich. $D_2O$ (99.9%) was purchased from Cambridge Isotope Laboratory, Inc. and used as received. AOT was purified by dissolving it in methanol and stirring the solution overnight in the presence of activated charcoal.[36] Subsequent filtration and removal of methanol by distillation under vacuum yielded AOT suitable for use. Doubly distilled deionized water was used throughout and prepared to a specific resistivity of >18 MΩ·cm (Barnstead E-pure system). Charcoal (Carbon, activated, coconut charcoal, 6−12 mesh) and NaOH were purchased from Fisher Scientific and used as received. HCl (hydrochloric acid, 37% ACS reagent grade) was purchased from Sigma-Aldrich.

A series of decavanadate, $V_{10}O_{28}^{6-}$ ($V_{10}$), stock solutions were prepared at 32.5, 12.2, 6.5, and 0.7 mM concentrations by dissolving $NaVO_3$ in doubly distilled deionized water in 90% of the desired volume in a volumetric flask, adjusting the pH to 3 by using 6 M HCl to form $V_{10}$, raising it back to pH 5.0 by using 1 M NaOH, and finally making up the required volume with doubly distilled deionized water. The 32.5, 12.2, and 6.5 mM stock solutions were used to make AOT RMs of $w_0 = 6$, 16, and 30, respectively; this protocol yielded RM solutions with constant overall $V_{10}$ concentration of 0.7 mM. For IR spectroscopy experiments, aqueous solutions were prepared by using 5% HOD in $H_2O$ and pure $H_2O$.

All solutions were freshly prepared just before spectral analysis. The pH values of the aqueous solutions were measured at 25 °C by using a pH meter (Orion 420A) calibrated with three buffers of pH 4, 7, and 10. The pH values were adjusted to within 0.05; pH variability between sample preparation and measurement was within 0.1 pH unit unless otherwise noted.

**II.B. RM Preparation and Characterization.** A 0.2 M AOT stock solution was prepared by dissolving AOT in isooctane under ambient conditions. Decavanadate ($w_0$ values of 6, 16, and 30) loaded RMs were prepared by pipetting a specific volume of aqueous $V_{10}$ stock solution into aliquots of the AOT stock solution. From the stock solution concentrations and given the aggregation numbers reported for AOT RMs,[36] we estimate 0.2 $V_{10}$ per RM with $w_0 = 6$, 0.8 $V_{10}$ per RM with $w_0 = 16$, and 2.2 $V_{10}$ per RM with $w_0 = 30$. All samples were mixed by vortexing 2−3 min prior to $^{51}V$ NMR spectroscopic measurements. The resulting solutions were transparent and yellow.

Dynamic light scattering (DLS) experiments were performed to identify the presence RMs in solution and to measure their size and polydispersity (DynaPro Titan, Wyatt). All measurements were performed at 25 °C. Viscosities used in the particle size calculations were obtained from experimental measurements of the samples by using Ubbeholde viscometers. For AOT concentrations at or below 0.2 M, viscosities were the same as that of pure isooctane within the error of the measurement. Sizes measured by using DLS were similar to those reported in the literature.[25,37–40] Samples were also characterized by their conductivity by using a conductivity meter (Orion 150A) equipped with a glass cell with two rectangular Pt electrodes (15 mm × 10 mm) with cell constant 0.1. The conductivity cell was calibrated with a standard 100 μS/cm solution.

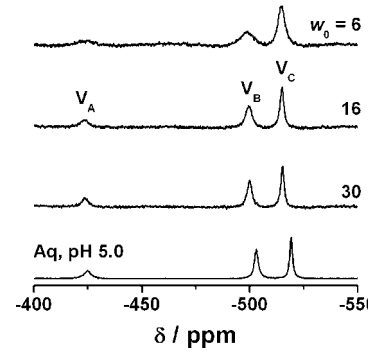


**Figure 2.** Representative $^{51}V$ NMR spectra of $V_{10}$ aqueous stock solution (0.7 mM at pH 5.0) and in AOT RMs with $w_0 = 6$, 16, and 30.

**II.C. $^{51}V$ NMR Spectroscopy.** $^{51}V$ NMR spectra were recorded by using Varian INOVA-300 MHz and INOVA-500 MHz spectrometers at 78.9 and 131.5 MHz, respectively. Spectra were acquired with a 83.6 kHz spectral window, a 60° pulse angle, and a 0.096 s acquisition time with no relaxation delay for the 300 MHz. For the 500 MHz spectrometer, spectra were acquired with a 39.2 kHz spectral window, a 60° pulse angle, and a 0.2 s acquisition time with no relaxation delay. $^{51}V$ chemical shifts were referenced against an external sample of $VO_4^{3-}$, which had been referenced against a sample of $VOCl_3$.[41,42] For peak position measurements, a 15 Hz exponential line broadening was applied before Fourier transformation. Longitudinal relaxation time ($T_1$) measurements were performed by using the inversion−recovery method with a spectral width of 6 kHz and an acquisition time of 2.7 s. The relative intensities of the vanadium oligomer signals were used to calculate the concentrations of decavanadate ($V_{10}$) and other oligomeric vanadates ($V_1$ monomer, $V_2$ dimer, $V_4$ tetramer, and $V_5$ pentamer).[42]

**II.D. Data Analysis.** The NMR FIDs collected were Fourier transformed and subjected to phase correction (MestReC V. 4.5.9.1 NMR data processing software for Windows). Resulting spectral peaks were fitted to find chemical shifts and line widths (OriginPro 7 and IgorPro, version 4.01).

Infrared vibrational spectra were collected with an FTIR Spectrophotometer (Nicolet, Magna 760). Individual spectra represent averages of 64 scans with 1.0 $cm^{-1}$ resolution. Samples were introduced by using an IR microvolume cuvette with KBr or $CaF_2$ windows and a 50 μm path length. Spectra were obtained for samples with pure water, with 5% HOD/$H_2O$, and with pure $H_2O$. This allowed us to explore the OD and OH stretching regions. To measure the spectrum that arises only from the OD stretching signal, spectra collected with $H_2O$ as the polar solvent were subtracted from the spectra of RMs containing 5%HOD/$H_2O$.

## III. Results

**III.A. $^{51}V$ NMR Measurements.** Figure 2 shows the $^{51}V$ NMR spectra for $V_{10}$ aqueous stock solution at pH 5.0 and $V_{10}$ in RM solutions with $w_0 = 6$, 16, and 30. Peak positions and line widths from analysis of the NMR data are summarized in Table 1. A complete listing of chemical shifts and line widths, which includes data from other $w_0$ values and data reported previously,[25] are included in Supporting Information. The

**TABLE 1: Chemical Shifts, Line Widths, and Spin-Lattice Relaxation Times ($T_1$) for the Three $^{51}V$ NMR Signals of $V_{10}$[a]**

| | $w_0$ | | | |
|---|---|---|---|---|
| | 6 | 16 | 30 | aqueous |
| | | Chemical Shift (ppm)[b] | | |
| $V_A$ | −421.6 ± 0.01 | −423.6 ± 0.4 | −423.6 ± 0.3 | −424.5 ± 0.4 |
| $V_B$ | −498.3 ± 0.003 | −499.7 ± 0.1 | −500.0 ± 0.1 | −501.6 ± 0.1 |
| $V_C$ | −514.4 ± 0.001 | −515.0 ± 0.4 | −515.3 ± 0.4 | −517.0 ± 0.4 |
| | | Line Width (Hz)[b] | | |
| $V_A$ | 1109 ± 82 | 582 ± 9.0 | 458 ± 26 | 503 ± 12 |
| $V_B$ | 835 ± 42 | 467 ± 59 | 350 ± 23 | 288 ± 4.0 |
| $V_C$ | 411 ± 52 | 266 ± 17 | 224 ± 11 | 203 ± 1.0 |
| | | $T_1$ (ms, measured) | | |
| $V_A$ | | −0.4 ± 0.01[c,d] | 0.66 | 0.66[b]; 0.6 ± 0.01[c,d] |
| $V_B$ | | 0.75[b]; 0.7 ± 0.01[c,d] | 1.14 | 1.24[b]; 1.1 ± 0.01[c,d] |
| $V_C$ | 0.95 | 1.49[b]; 1.3 ± 0.003[c,d] | 1.81 | 1.88[b]; 1.8 ± 0.03[c,d] |
| | | $T_1$ (ms, from $\Delta_{1/2}$)[e] | | |
| $V_A$ | 0.31 | 0.54[b]; 0.5 ± 0.1[c,d] | 0.65 | 0.64[b]; 0.6 ± 0.03[c,d] |
| $V_B$ | 0.36 | 0.59[b]; 0.6 ± 0.02[c,d] | 0.85 | 1.09[b]; 1.0 ± 0.01[c,d] |
| $V_C$ | 0.72 | 1.12[b]; 1.1 ± 0.02[c,d] | 1.35 | 1.58[b]; 1.5 ± 0.01[c,d] |
| | | Number of V Atom/RM | | |
| | 2 | 8 | 22 | |
| | | Number of $V_{10}$/RM | | |
| | 0.2 | 0.8 | 2.2 | |

[a] Measurements performed in triplicate and standard deviations indicated. All RM solutions were made by using 0.2 M AOT/isooctane and a 0.7 mM pH 5.0 ± 0.05 aqueous $V_{10}$ stock solution. [b] This work. [c] From ref 31. [d] 10 mM $V_{10}$ at pH 4.9 ± 0.05 and corresponding RM samples (0.5 M AOT/isooctane). [e] Assuming no line broadening due to dynamic process and $1/T_2^* = 1/T_2$, $T_2^* \approx T_2$, and $T_2 \approx T_1$. $T_1$ values calculated from line width ($\Delta_{1/2} = 1/\pi T_2^*$).

concentration of the aqueous $V_{10}$ solution, as described in Section II.B, ensured that most RMs encapsulated at least one $V_{10}$ molecule.

Several features in the spectra shown in Figure 2 demonstrate differences between bulk aqueous solution and the environment found in the RMs. For example, the peak positions for features corresponding to the three different $V_{10}$ atoms, $V_A$, $V_B$, and $V_C$, appear at different chemical shifts in RM and aqueous bulk solution. These results agree with data that we have reported previously.[31] Careful fitting of the peaks reveal that all three $V_{10}$ signals display a consistent downfield shift with increasing RM size, as shown in Figure 3. These chemical shifts show a trend toward bulk water behavior of the RM water pool but never reach the same chemical shift as the $V_{10}$ in bulk solution, even in the largest RM probed, $w_0 = 30$, where the RM should contain enough water molecules to appear bulk-like.[43] The chemical shifts for the RM samples always differ from the aqueous stock sample.

In addition to the changes seen in chemical shifts, spectra in Figure 2 show dramatic differences in the $^{51}V$ NMR line widths for the $V_{10}$ in the RMs compared to the aqueous stock solution. Specifically, the line widths increase with decreasing RM size. The changes in line width are summarized in Table 1. We observed the most dramatic line broadening for the $V_A$ feature, but all three lines broaden as the RM size decreases. For a RM of $w_0 = 30$, the line widths approach those of the bulk solution. At $w_0 = 6$, the observed line widths for $V_B$ and $V_C$ are 2−3 times greater than the line widths measured in the aqueous stock solution at pH 5.0; the signal for $V_A$ has broadened to the extent of barely being distinguishable from the baseline.

Knowing the spin−lattice relaxation times, $T_1$, allows us to interpret the source of line broadening in our samples. $T_1$ measurements were attempted for all samples probed; where we could obtain them, $T_1$ values are given in Table 1 and in the Supporting Information. In bulk aqueous solution, $T_1$ values could be measured for each different vanadium signal in $V_{10}$. Although we could obtain $T_1$ values for $V_{10}$ in the largest RMs probed, decreasing $w_0$ diminished the value $T_1$ to the point where it was no longer measurable with the spectrometer used. Because spin−lattice relaxation contributes to the NMR line width, the shorter $T_1$ values could account for line broadening in the $^{51}V$ NMR spectra. The significant decrease in $T_1$ with decreasing RM size could reflect changes in viscosity, because relaxation depends on the ability of the molecule to move.[44,45] Literature reports that with decreasing temperature, the line width increases, and $T_1$ decreases, consistent with increasingly limited mobility as the sample cools.[46] Our observations of decreasing $T_1$ and increasing line width suggest similar decreases in $V_{10}$ mobility in the RMs.

To explore the nature of the observed $^{51}V$ NMR line broadening, we have fitted all of the NMR spectral peaks to determine their line shapes. By investigating whether the spectral peaks fit best to a Lorentzian, Gaussian, or Voigt (convolution between Lorentzian and Gaussian) line profile, we aimed to gauge the degree of inhomogeneous line broadening in the spectral features. We find that in bulk aqueous solution, the spectral peaks all fit well to Lorentzian line shapes. However, signals for $V_A$ and $V_C$ in the RMs require a Voigt line shape to accurately fit the signals. At the same time, the $V_B$ feature remains relatively Lorentzian in shape.

**III.B. Infrared Spectroscopy.** Figure 4 shows IR spectra in the OD stretching region for various small RMs prepared with 5% HOD in $H_2O$. Because it is essentially a local mode rather than a normal mode, the OD stretching mode in HOD is much less complicated than the $H_2O$ stretch spectral region, which includes a combination of symmetric and antisymmetric stretching features or the Fermi resonance with the bend overtone. These spectra neatly demonstrate qualitative features of the water found inside the RMs. Figure 4 displays significant spectral shifting and broadening of the OD peak for RMs with $w_0 = 6$ containing $V_{10}$ compared to those with only water. Indeed, the spectrum of the $w_0 = 6$ RM containing $V_{10}$ nearly

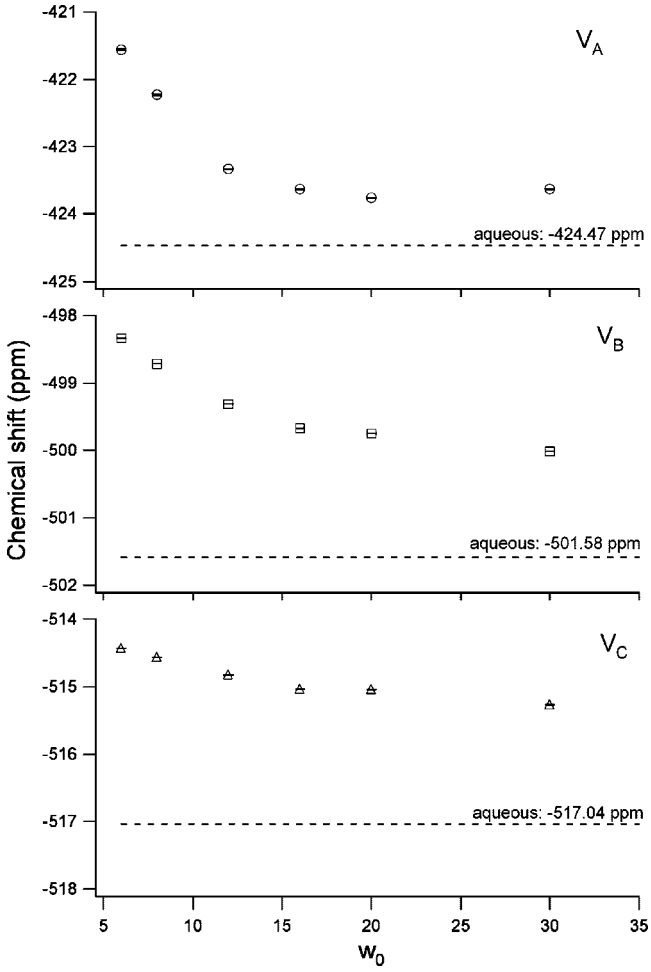


**Figure 3.** Chemical shifts for $V_{10}$ atoms in AOT RMs as a function of RM size obtained by fitting spectral peaks.

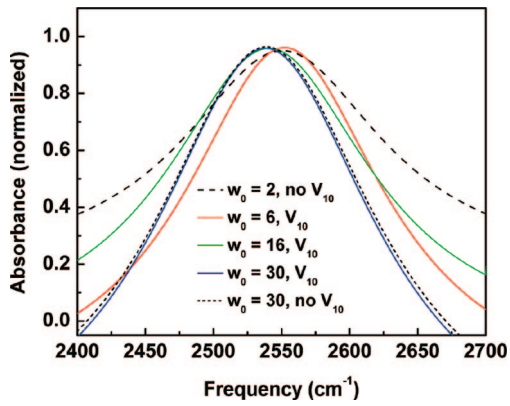


**Figure 4.** Background-subtracted FTIR absorption spectra of the OD stretch mode of 5% HOD in different size RMs.

overlays the spectrum of the $w_0 = 2$ containing only water. Because virtually all the water in the $w_0 = 2$ RM contacts the interfacial region, its similarity to the spectrum of the $w_0 = 6$ RM containing $V_{10}$ suggests significant perturbation of the water in the $w_0 = 6$ RM containing $V_{10}$.

## IV. Discussion

In general, researchers agree that the water found inside RMs differs from bulk water.[21,24,47–53] However, the nature of the deviation varies depending on the methods by which the systems are investigated. The results presented above suggest a number of ways that the water in the RMs departs from bulk behavior. We have observed the changes in chemical shift for all three signals of $V_{10}$ molecule upon encapsulation in the RMs.[31] $V_{10}$ protonation is highly sensitive to solution acidity/basicity, as shown in eqs 1–3. The $^{51}V$ NMR spectrum of $V_{10}$ shifts depending on protonation state, displaying the proton equilibria, are shown in eq 1–3.[34]

$$V_{10}O_{28}^{6-} + H^+ \rightleftharpoons HV_{10}O_{28}^{5-} \qquad pK_1 = 5.5 - 6.0 \qquad (1)$$

$$HV_{10}O_{28}^{5-} + H^+ \rightleftharpoons H_2V_{10}O_{28}^{4-} \qquad pK_2 = 3.1 - 3.7 \qquad (2)$$

$$H_2V_{10}O_{28}^{4-} + H^+ \rightleftharpoons H_3V_{10}O_{28}^{3-} \qquad pK_3 \approx 2.0 \qquad (3)$$

Changes in the local apparent pH can be monitored through the NMR chemical shifts. In the pH = 5 solutions used to create RMs, the dominant species was $HV_{10}O_{28}^{5-}$. The significant changes in chemical shifts observed when $HV_{10}O_{28}^{5-}$ was solubilized in the RM is consistent with its deprotonation upon introduction to the RM interior as we have observed previously.[31] As data in Figure 3 display, even in the largest RM, $w_0$ =30, the chemical shifts differ from that in bulk aqueous solution. We have attributed this consistent departure from bulk solvation to the deprotonation of the $V_{10}$ species inside the RMs. These changes support the interpretation that the molecule is in a different environment from its bulk situation. In particular, the changes in $V_{10}$ chemical shift from aqueous to RM environments reflect the propensity for the $H^+$ to migrate to the interface with a concomitant motion of $Na^+$ counterions of the AOT surfactant to move to the interior water pool.[31]

The line width and $T_1$ values for the $^{51}V$ NMR signals of $V_{10}$ also indicate differences between bulk aqueous solutions and the environment inside the RMs. Specifically, the line widths increase as a function of decreasing $w_0$. Additionally, the $T_1$ values decrease with decreasing $w_0$. Both line width and $T_1$ are associated with the relaxation processes for the $V_{10}$ molecule.[33,54,55] As relaxation speeds up, line width increases, and $T_1$ decreases. Thus, the observed line width and $T_1$ values measured suggest that as the micelle size decreases, the RM environment provides an increasingly efficient path for the $V_{10}$ molecules to relax, most likely because of increasing interactions between the probe and the surrounding.

In the limit where the spin−lattice relaxation ($T_1$) approximates the spin−spin relaxation ($T_2$), direct inversion of the spectral line width should approximately equal to the measured value for $T_1$, that is

$$T_1 \approx T_2^* \approx \frac{1}{\pi\Gamma} \qquad (4)$$

where $\Gamma$ is the full width at half height in Hertz. Data in Table 1 show that this relation holds for signals in bulk aqueous solution. This suggests that the spectral lines reflect homogeneous broadening without substantial contributions from the environment. For the RM spectral peaks where we could measure $T_1$, we find that the signals are no longer in the motional limit where $T_1 \approx T_2^*$, even for the largest RMs examined, which by other measures are described as bulk-like. For the smaller RMs, substantial inhomogeneities in the environment undoubtedly contribute to changing the signals, adding spectral breadth and precluding measurement of $T_1$.

A number of possible scenarios could explain the observed trends in the lifetimes and measured NMR line shapes of the three different vanadium atoms in the $V_{10}$ molecule ($V_A$, $V_B$, and $V_C$), including effects of polydispersity of RM sizes, constrained motion of the $V_{10}$ in the RMs, deformation of the

$V_{10}$ electron cloud or structure, and movement of the $V_{10}$ through inhomogeneous environments in the RMs. To explore the validity of these interpretations, we have simulated their effects through a simple empirical model based on our NMR spectra. We apply this model to the different effects that could be associated with chemical shifts and line broadening.

In the simplest case, the line broadening observed in the $^{51}V$ NMR spectrum of $V_{10}$ would arise from homogeneous lifetime broadening. This would lead the spectra to reflect the motional limit where $1/T_1 \approx 1/T_2$.[54] As we note above, this is true for $V_{10}$ in aqueous solution but not in the RMs. Thus, our model starts by creating a NMR spectrum for each V peak at each $w_0$ in the motional limit; to this model, we introduce broadening through various effects such as inhomogeneous environment, constrained motion, and so forth, and compare the resulting spectral features to the experimentally measured lines. In this way, we hope to identify which broadening processes are responsible for the observed spectra.

In the motional limit, the intensity at frequency $\nu$ follows a Lorentzian distribution.[54] By using the Lorentzian line width obtained from the Lorentzian portion of the Voigt fit to the data, as described above, we generated a hypothetical $T_1$ value. We empirically fit the measured lifetimes and chemical shifts to obtain the size dependencies to

$$T_1(\text{V atom}) = c_1(\text{V atom}) - c_2(\text{V atom}) \times \exp(-c_3(\text{V atom})w_0) \quad (5)$$

$$\delta(\text{V atom}) = c_4(\text{V atom}) \exp(-c_5(\text{V atom})w_0) - \nu(\text{V atom}) \quad (6)$$

where V atom refers to $V_A$, $V_B$, or $V_C$, $c_1$, $c_2$, $c_3$, $c_4$, and $c_5$ are empirically determined constants and $\nu$ is the center frequency of the spectral feature. A gamma distribution was then used to generate a simulated population of RMs based on the average size and standard deviation, as measured by DLS. To obtain a simulated spectrum for the entire distribution of RM sizes, we calculated the predicted Lorentzian line width according to

$$\varphi(\nu) \approx \frac{T_1}{1 + T_1^2(\nu - \delta)^2} \quad (7)$$

which was multiplied by the relative population at each size. To obtain the final simulated spectrum for any particular $w_0$ value, all the spectra were summed together. Although this simulation does not provide a quantitative estimate of the spectra, we can use it to explore the impact of various broadening mechanisms.

First, we consider the effects of RM size dispersity on $V_{10}$ line width and $T_1$. As seen in Table 1, both $T_1$ and line width, $\Delta$, are affected by RM size. When we develop interpretations for the RM data, it is usually on the basis of some average RM size, even though the quantities measured in experiments represent average values for an ensemble of RMs with a distribution of sizes. Because $T_1$ and line width depend on RM size, polydispersity in RM size could result in inhomogeneous broadening of the NMR peaks. Although data in the literature suggest that AOT RMs have relatively low size polydispersity,[56–60] it is possible that the introduction of the $V_{10}$ to the RM interior causes more dispersity. We simulate the effect of size polydispersity by generating a range of NMR spectral signals and adding them together in a weighted average. We expect to observe a larger effect from polydispersity in smaller RMs because the size dependences of $T_1$ and $\Delta$ are greater at smaller $w_0$. In all cases, the simulated spectra displayed peaks with narrower line widths than those in experimental spectra, and moreover, the simulated peaks remained Lorentzian regardless of average $w_0$, suggesting that size polydispersity does not lead to significant inhomogeneous broadening. Although it may lead to peaks with artificially narrow line widths, the motional narrowing approximation used in the simulation does not account for the disagreement in line shape between experiment and simulation. Specifically, experimental peaks require a Voigt profile to fit, whereas the simulated peaks retain a Lorentzian shape regardless of the parameters. This leads us to conclude that RM size polydispersity is not the dominant cause of inhomogeneous broadening in the smaller RMs.

A second possible source of line broadening is if the $V_{10}$ motion is restricted along specific axes through interfacial interactions or confinement by the RM. Because vanadium (V) is quadrupolar, its line width is exclusively sensitive to restricted motion, resulting in inhomogeneous broadening.[61,62] Thus, if the $V_{10}$ displayed preferential rotation about a specific axis, we might expect to observe unequal broadening between the various different vanadium atoms in the complex. For example, as RM diameter decreases, the long axis of the molecule (Figure 1) should be geometrically constrained before the other axes. In the extreme case, $V_{10}$ could spin relatively freely about the long axis; yet, the confinement by the RM environment could prevent reorientation of this axis. However, strong interaction of the $V_{10}$ by the RM should lead the $V_{10}$/AOT NMR spectra to broaden much more dramatically that what is observed here. Yet, without interfacial contact, there is little to prevent $V_{10}$ from tumbling isotropically. Furthermore, the intermediate axis of $V_{10}$ (containing the four $V_C$ atoms) is almost the same length as the long axis, 7.7 versus 8.3 Å, and should be nearly as confined as the long axis. If $w_0$ is sufficiently small to constrain the long axis on the basis of size alone, the intermediate axis would likewise be confined, largely eliminating rotation by the molecule. The fact that the NMR peaks of $V_B$ atoms remain predominantly Lorentzian at small $w_0$ whereas the $V_A$ and $V_C$ peaks require a Voigt challenges the validity of this hypothesis.

Finally, we consider the inhomogeneity of the environment within the RMs. The medium that surrounds $V_{10}$ in the RM interior differs from the interfacial region.[24,31] Although the core-interior water possesses some bulk-like properties, water at the interface displays slower reorientation, most likely because of interactions with the surface headgroups and counterions.[24,63] As $V_{10}$ moves in the RM, it can sample the interfacial region. Because the surface area represents a larger fraction in the small RMs than in the large ones, statistically, we expect $V_{10}$ to spend significantly more time near the interface in a small RM than in a large RM. NMR measures an ensemble of $V_{10}$ molecules; therefore, at any given time, some molecules are within the RM core whereas some are in the shell. Because of the sensitivity of quadrupolar atoms to their environment, these different environments result in peak broadening, which is more noticeable when the shell occupies a greater percentage of the RM (when $w_0$ is small). We conclude that this interpretation is the most reasonable explanation for our observations and is consistent with the common interpretation of line broadening in homogeneous media.

Researchers have applied a range of methods to investigate the nature of water inside AOT RMs.[64,65] A picture has emerged in which the water molecules near the surfactant head groups interacting with the head groups as well as the associated sodium counterions cause disruption of the normal water hydrogen bonding. A ~5 Å layer of shell, water exists at the interface with properties different from bulk water.[24,25] In contrast, the

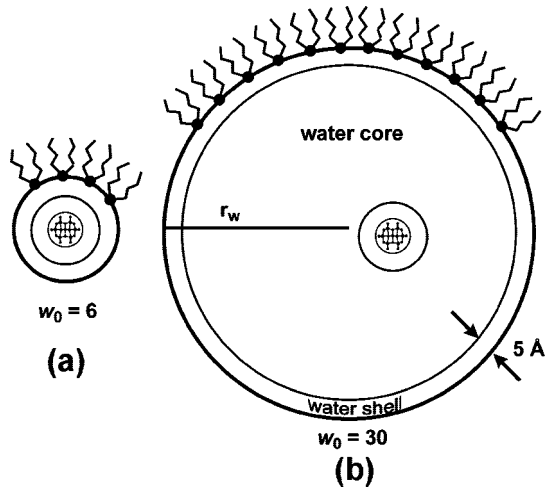


**Figure 5.** Schematic illustration of RMs with $w_0 = 6$ (a) and $w_0 = 30$ (b) AOT RMs (only a few surfactant molecules are shown in both RMs for clarity). The water pool radius ($r_w$) for AOT $w_0 = 30$ is ~50 Å and 14 Å for $w_0 = 6$. The shell thickness is shown to be 5 Å.[24] The two long axes for $V_{10}$ molecule are 7.7 and 8.3 Å.

water molecules in the core of the water pool of larger RMs ($w_0 > 10$) are reported to possess properties like those of bulk water.[24] In the studies reported here, signal broadening and changes in signal lifetimes in $^{51}V$ NMR spectra for $V_{10}$ in RMs are consistent with the probe interacting with the interfacial water layer.[64,66]

To test this hypothesis, we have measured IR vibrational spectra of the water in $V_{10}$-containing RMs. The degree of hydrogen bonding or its disruption can be observed in these spectra. The OD stretching vibration can effectively be modeled as being due to a linear sum of core bulk-like water and shell interfacial water, which has been approximated by the spectrum obtained for $w_0 = 2$ RMs.[24] As shown in Figure 4, when the RMs encapsulate $V_{10}$, the spectrum peaks at a higher frequency than in the absence of $V_{10}$. Indeed, the $V_{10}$-containing RMs peak at almost the same frequency as the $w_0 = 2$ spectrum. The intramicellar water appears to gain more shell water at the expense of the core water, virtually eliminating contribution from the bulk-like core water. In a small RM, essentially all the water is shell water.

When we place $V_{10}$ molecules in RMs with $w_0 < 10$, very little space is left inside the RMs for the $V_{10}$ (Figure 5). Indeed, RMs with $w_0 = 6$ have internal diameters of ~28 Å. Excluding the shell water that hydrates the interior interface of the RM, ~5 Å, leaves a ~18 Å diameter water core. Given that the dimensions of the $V_{10}$ molecule are $8.3 \times 7.7 \times 5.4$ Å$^3$, an 18 Å diameter should provide sufficient volume for the $V_{10}$ molecule to move freely in the water pool. However, the IR spectra suggest that no bulk-like water exists in this environment, and the $^{51}V$ NMR spectra for $w_0 = 6$ samples have substantially broadened peaks. This suggests that the solvation of the $V_{10}$ complex with its sodium counterions accounts for much of the shell water. Indeed, adding a single shell of water that is ~5 Å thick (similar to the RM shell) to the $V_{10}$ would lead its long dimension to be ~18 Å, not including the hydrated $Na^+$ counterions, as depicted in Figure 5a. Thus, it appears that each $V_{10}$ molecule has its own water shell with properties that differ dramatically from bulk water.

In larger RMs, the effect of confinement becomes less pronounced. Water molecules interacting with surfactant headgroups account for less than half the intramicellar water.[24] The substantial negative charge on the $V_{10}$ molecules should lead them to reside away from the negatively charged RM interface. The internal diameter of a large RM, such as $w_0 = 30$, is ~100 Å, which, when excluding the shell of 5 Å from the inner surface, leaves a ~90 Å diameter cavity inside the RM. We estimate that an average of two $V_{10}$ molecules will occupy this ~90 Å diameter cavity in the $w_0 = 30$ RMs. Although it would appear that this environment should provide ample room for the $V_{10}$ molecule to tumble freely as it can in bulk water, the line shape and $T_1$ data suggest that differences continue to exist for this environment. It is possible that the additional $Na^+$ ions along with their solvation shell could impact the local environment around the $V_{10}$ and that this difference in $H^+$ activity is contributing to the observed changes in the water. Indeed, water dynamics are slower in the solvation sphere of a sodium cation.[67]

Finally, when the RM interior approaches the size of the solvated $V_{10}$ molecule, RMs are no longer stable. That is, our attempts to create AOT RMs encapsulating $V_{10}$ with $w_0$ lower than 6 lead to phase separation or precipitation of the $V_{10}$. Thus, it appears that $V_{10}$ requires a layer of water ~5 Å thick to solvate it. Any structures lacking this solvation sphere are not sufficiently stable to remain emulsified.

## V. Conclusions

Here, we present results from experiments investigating the properties of water in AOT RMs encapsulating the large decavanadate, $V_{10}$, probe molecule. The combination of $^{51}V$ NMR and steady-state IR spectroscopies allows us to measure how the $V_{10}$ probe molecule impacts the intramicellar environment water. The NMR spectra show that the intramicellar environment of an aqueous solution of triprotonated $V_{10}$ leads to deprotonation of the molecule; the reverse micellar interior is more basic than the acidic solutions from which the RMs were formed. It also shows that the confined environment around the $V_{10}$ molecule hinders its motion. This is not surprising in small RMs. However, even in large RM, $V_{10}$ behave differently than in bulk solution. For the smallest RMs containing $V_{10}$, it is found in a highly confined environment. IR spectroscopy of the water in these systems shows that the $V_{10}$ molecule interacts with water, disrupting its hydrogen bonding. In the $w_0 = 6$ RMs, virtually all of the water is perturbed either by the inner surface of the micelle interface or by the $V_{10}$ probe. RM sizes smaller than $w_0 = 6$ preclude formation of hydration of the RM interior interface and a hydration shell around the $V_{10}$ probe, leading either the solutions to phase separate or the probe to precipitate out from the solution. This result supports the interpretation that $V_{10}$ requires a certain hydration shell as solvation before promotion of RM formation. These results show the interactions of water with a molecular probe and highlights how the probe can affect the properties of water in confined environments. The subtle effects of $H^+$ activity in these RMs may partly be responsible for determining whether the water appears bulk-like or not.

**Acknowledgment.** This material is based upon work supported by the National Science Foundation under Grant no. 0628260. We thank Prof. Ellen Fisher for the use of her FTIR spectrometer.

**Supporting Information Available:** This material is available free of charge via the Internet at http://pubs.acs.org.

## References and Notes

(1) Falcone, R. D.; Biasutti, M. A.; Correa, N. M.; Silber, J. J.; Lissi, E.; Abuin, E. *Langmuir* **2004**, *20*, 5732–5737.

(2) Martinek, K.; Levashov, A. V.; Klyachko, N. L.; Khmelnitski, Y. L.; Berezin, Y. V. *Eur. J. Biochem.* **1986**, *155*, 453–468.
(3) Gebicka, L.; Jurgas-Grudzinska, M. *Z. Naturforsch.* **2004**, *59*, 887–891.
(4) Durfor, C. N.; Bolin, R. J.; Sugasawara, R. J.; Massey, R. J.; Jacobs, J. W.; Schultz, P. G. *J. Am. Chem. Soc.* **1988**, *110*, 8713–8714.
(5) Menger, F. M.; Yamada, K. *J. Am. Chem. Soc.* **1979**, *101*, 6731–6734.
(6) Correa, N. M.; Durantini, E. N.; Silber, J. J. *J. Org. Chem.* **1999**, *64*, 5757–5763.
(7) Correa, N. M.; Durantini, E. N.; Silber, J. J. *J. Org. Chem.* **2000**, *65*, 6427–6433.
(8) Correa, N. M.; Zorzan, D. H.; Chiarini, M.; Cerichelli, G. *J. Org. Chem.* **2004**, *69*, 8224–8230.
(9) Correa, N. M.; Zorzan, D. H.; D.; Anteo, L.; Lasta, E.; Chiarini, M.; Cerichelli, G. *J. Org. Chem.* **2004**, *69*, 8231–8438.
(10) Fernandes, M. L. M.; Krieger, N.; Baron, A. M.; Zamora, P. P.; Ramos, L. P.; Mitchell, D. A. *J. Mol. Catal. B: Enzym.* **2004**, *30*, 43–49.
(11) Pal, T.; De, S.; Jana, N. R.; Pradhan, N.; Mandal, R.; Pal, A.; Beezer, A. E.; Mitchell, J. C. *Langmuir* **1998**, *14*, 4724–4730.
(12) Naoe, K.; Murata, M.; Ono, C.; Kawagoe, M.; Imai, M. *Biochem. Eng. J.* **2002**, *10*, 137–142.
(13) Faeder, J.; Ladanyi, B. M. *J. Phys. Chem. B* **2005**, *109*, 6732–40.
(14) Abuin, E.; Lissi, E.; Solar, C. *J. Colloid Interface Sci.* **2005**, *283*, 87–93.
(15) Piletic, I. R.; Tan, H. S.; Fayer, M. D. *J. Phys. Chem. B* **2005**, *109*, 21273–21284.
(16) Tan, H. S.; Piletic, I. R.; Fayer, M. D. *J. Chem. Phys.* **2005**, *122*, 174501–174509.
(17) Tan, H. S.; Piletic, I. R.; Riter, R. E.; Levinger, N. E.; Fayer, M. D. *Phys. Rev. Lett.* **2005**, *94*, 057405/1–057405/4.
(18) Riter, R. E.; Willard, D. M.; Levinger, N. E. *J. Phys. Chem. B* **1998**, *102*, 2705–2714.
(19) Sando, G. M.; Dahl, K.; Owrutsky, J. C. *J. Phys. Chem. B* **2005**, *109*, 4084–4095.
(20) Abel, S.; Sterpone, F.; Bandyopadhyay, S.; Marchi, M. *J. Phys. Chem. B* **2004**, *108*, 19458–19466.
(21) Faeder, J.; Ladanyi, B. M. *J. Phys. Chem. B* **2000**, *104*, 1033–1046.
(22) Hasegawa, M.; Sugimura, T.; Suzaki, Y.; Shindo, Y.; Kitahara, A. *J. Phys. Chem.* **1994**, *98*, 2120–2124.
(23) Hirose, Y.; Yui, H.; Sawada, T. *J. Phys. Chem. B* **2004**, *108*, 9070–9076.
(24) Piletic, I. R.; Moilanen, D. E.; Spry, D. B.; Levinger, N. E.; Fayer, M. D. *J. Phys. Chem. A* **2006**, *110*, 4985–4999.
(25) Maitra, A. *J. Phys. Chem.* **1984**, *88*, 5122–5125.
(26) Willard, D. M.; Riter, R. E.; Levinger, N. E. *J. Am. Chem. Soc.* **1998**, *120*, 4151–4160.
(27) Nandi, N.; Bhattacharyya, K.; Bagchi, B. *Chem. Rev.* **2000**, *100*, 2013–2046.
(28) Heitz, M. P.; Bright, F. V. *Appl. Spectrosc.* **1996**, *50*, 732–739.
(29) Sando, G. M.; Zhong, Q.; Owrutsky, J. C. *J. Chem. Phys.* **2004**, *121*, 2158–2168.
(30) Piletic, I. R.; Moilanen, D. E.; Levinger, N. E.; Fayer, M. D. *J. Am. Chem. Soc.* **2006**, *128*, 10366–10367.
(31) Baruah, B.; Roden, J. M.; Sedgwick, M.; Correa, N. M.; Crans, D. C.; Levinger, N. E. *J. Am. Chem. Soc.* **2006**, *128*, 12758–12765.
(32) Baruah, B.; Crans, D. C.; Levinger, N. E. *Langmuir* **2007**, *23*, 6510–6518.
(33) Crans, D. C.; Baruah, B.; Levinger, N. E. *Biomed. Pharmacother.* **2006**, *60*, 174–181.
(34) Howarth, O. W.; Jarrold, M. *J. Chem. Soc., Dalton Trans.* **1978**, 503–506.
(35) Crans, D. C.; Smee, J. J.; Gaidamauskas, E.; Yang, L. *Chem. Rev.* **2004**, *104*, 849–902.
(36) Chowdhury, P. K.; Ashby, K. D.; Dutta, A.; Petrich, J. W. *Photochem. Photobiol.* **2000**, *72*, 612–618.
(37) Bohidar, H. B.; Behboudnia, M. *Colloids Surf., A* **2001**, *178*, 313–323.
(38) Zulauf, M.; Eicke, H.-F. *J. Phys. Chem.* **1979**, *83*, 480–486.
(39) Andrews, B. A.; Pyle, D. L.; Asenjo, J. A. *Biotechnol. Bioeng.* **1994**, *43*, 1052–1058.
(40) Spirin, M. G.; Brichkin, S. B.; Razumov, V. F. *Zh. Nauch. Prikl. Fotog.* **2000**, *45*, 20–27.
(41) Crans, D. C.; Shin, P. K. *Inorg. Chem.* **1988**, *27*, 1797–1806.
(42) Crans, D. C.; Rithner, C. D.; Theisen, L. A. *J. Am. Chem. Soc.* **1990**, *112*, 2901–2908.
(43) Izquierdo, C.; Moya, M. L.; Usero, J. L.; Casado, J. *Monatsh. Chem.* **1992**, *123*, 383–389.
(44) Peterson, R. W.; Lefebvre, B. G.; Wand, A. J. *J. Am. Chem. Soc.* **2005**, *127*, 10176–10177.
(45) Nimtz, G.; Weiss, W. *Z. Phys. B: Condens. Matter* **2005**, *67*, 483–487.
(46) Domaille, P. J. *J. Am. Chem. Soc.* **1984**, *106*, 7677–7687.
(47) Douhal, A.; Angulo, G.; Gil, M.; Organero, J. A.; Sanz, M.; Tormo, L. *J. Phys. Chem. B* **2007**, *111*, 5487–5493.
(48) Volkov, V. V.; Palmer, D. J.; Righini, R. *J. Phys. Chem. B* **2007**, *111*, 1377–1383.
(49) Volkov, V. V.; Palmer, D. J.; Righini, R. *Phys. Rev. Lett.* **2007**, *99*, 078302.
(50) Dokter, A. M.; Woutersen, S.; Bakker, H. J. *Proc. Natl. Acad. Sci. U. S. A.* **2006**, *103*, 15355–15358.
(51) Balasubramanian, S.; Pal, S.; Bagchi, B. *Phys. Rev. Lett.* **2002**, *89*, 115505.
(52) Novaki, L. P.; El Seoud, O. A. *J. Colloid Interface Sci.* **1998**, *202*, 391–398.
(53) Onori, G.; Santucci, A. *J. Phys. Chem. B* **1993**, *97*, 5430–5434.
(54) Farrar, T. C.; Becker, E. D. *Pulse and Fourier transform NMR; introduction to theory and methods*; Academic Press: New York, 1971.
(55) Sandstrom, J. *Dynamic NMR Spectroscopy*; Academic Press: New York, 1982.
(56) Simmons, B.; Agarwal, V.; McPherson, G.; John, V.; Bose, A. *Langmuir* **2002**, *18*, 8345–8349.
(57) Freeman, K. S.; Beck Tan, N. C.; Trevino, S. F.; Kline, S.; McGown, L. B.; Kiserow, D. J. *Langmuir* **2001**, *17*, 3912–3916.
(58) Arleth, L.; Pedersen, J. S. *Phys. Rev. E: Stat. Nonlin., Soft Matter Phys.* **2001**, *63*, 061406.
(59) Amararene, A.; Gindre, M.; Le Huerou, J.; Urbach, W.; Valdez, D.; Waks, M. *Phys. Rev. E: Stat. Phys., Plasmas, Fluids* **2000**, *61*, 682–689.
(60) Kotlarchyk, M.; Chen, S.-H. *J. Chem. Phys.* **1983**, *79*, 2461–2469.
(61) Butler, A.; Eckert, H. *J. Am. Chem. Soc.* **1989**, *111*, 2802–2809.
(62) Saponja, J. A.; Vogel, H. J. *J. Inorg. Biochem.* **1996**, *62*, 253–270.
(63) Harpham, M. R.; Ladanyi, B. M.; Levinger, N. E. *J. Phys. Chem. B* **2005**, *109*, 16891–16900.
(64) Silber, J. J.; Biasutti, A.; Abuin, E.; Lissi, E. *Adv. Colloid Interface Sci.* **1999**, *82*, 189–252.
(65) De, T. K.; Maitra, A. *Adv. Colloid Interface Sci.* **1995**, *59*, 95–193.
(66) Hunt, N. T.; Jaye, A. A.; Meech, S. R. *Chem. Phys. Lett.* **2005**, *416*, 89–93.
(67) Zhu, S. B.; Robinson, G. W. *J. Chem. Phys.* **1992**, *97*, 4336–4348.

JP800390T